Journal of
Applied Remote Sensing

# Comparative analysis of classification algorithms and multiple sensor data for land use/land cover classification in the Brazilian Amazon

Guiying Li
Dengsheng Lu
Emilio Moran
Sidnei João Siqueira Sant'Anna

SPIE

# Comparative analysis of classification algorithms and multiple sensor data for land use/land cover classification in the Brazilian Amazon

**Guiying Li,[a] Dengsheng Lu,[b] Emilio Moran,[a] and Sidnei João Siqueira Sant'Anna[c]**

[a]Indiana University, Anthropological Center for Training and Research on Global Environmental Change, Bloomington, Indiana 47405

[b]Michigan State University, Center for Global Change and Earth Observations, 1405 S. Harrison Road, East Lansing, Michigan 48823

ludengsh@msu.edu

[c]National Institute for Space Research, Av. dos Astronautas, 1758, 12245-010 São Jose dos Campos, SP, Brazil

**Abstract.** A comparative analysis of land use/land cover (LULC) classification results in the Brazilian Amazon based on four classification algorithms and four remote sensing datasets was conducted in order to better understand the selection of a classification algorithm suitable for a specific remote sensing data. It is shown that maximum likelihood classifier (MLC) provided reasonably good classification accuracy when Landsat Thematic Mapper (TM) or the TM and Advanced Land Observing Satellite Phased Array type L-band Synthetic Aperture Radar (ALOS PALSAR) data-fusion images were used, but nonparametric algorithms such as classification tree analysis for TM multispectral bands and K-nearest neighbor for the combination of TM and PALSAR data provided better classification than MLC. Individual PALSAR dataset is not suitable for detailed LULC classification and has much poorer classification accuracy (47.6% to 59.4%) than Landsat TM image (79.7% to 84.9%). However, integration of TM and PALSAR data through the wavelet-merging technique improved classification accuracy. It is implied that the importance of selecting a suitable classification algorithm for a specific dataset by considering such factors as overall classification accuracy and time and labor involved in a classification procedure. Important information for guiding the selection of remote sensing dataset and associated classification algorithms for LULC classification in the moist tropical regions is also provided.  [DOI: 10.1117/1.JRS.6.061706]

**Keywords:** Landsat; radar; land use/cover classification; Brazilian Amazon.

Paper 12214SS received Jul. 18, 2012; revised manuscript received Nov. 24, 2012; accepted for publication Nov. 27, 2012; published online Dec. 14, 2012.

## 1 Introduction

Land use/land cover (LULC) classification is one of the most important applications in remote sensing, but is a complex procedure, because different factors, such as the spatial resolution of the remotely sensed data, availability of different data sources (e.g., field survey data, digital elevation model data), a suitable LULC classification system, availability of classification software, and the analyst's experience may affect the classification results.[1] The difficulty in identifying an optimal classification method for a specific study often requires conducting a comparative study of different classifiers in order to generate a satisfied classification.[2–4] Therefore, which classification algorithm should be used for a specific dataset in a study area remained to be answered, although many classification methods, from traditional parametric algorithms such as maximum likelihood classifier (MLC), to advanced nonparametric algorithms such as artificial neural network (ANN), decision tree, and support vector machine (SVM) are available.[1,5] Another challenge is to select a proper dataset for LULC classification. However, different kinds of sensor data have various

0091-3286/2012/$25.00 © 2012 SPIE

characteristics in spatial, spectral, radiometric, and temporal resolutions, as well as different angles and polarizations for radar data. It is important to effectively incorporate different data features into a classification procedure for improving LULC classification accuracies.[1]

For a specific LULC classification, selection of a suitable remote-sensing dataset and selection of a suitable algorithm for the specific dataset are two critical issues but have not been fully examined. Lu and Weng[1] had summarized the major classification algorithms and discussed the potential techniques to improve LULC classification. Thanks to support from the U.S. National Science Foundation for a research project entitled "Advancing Land Use and Land Cover Analysis by Integrating Optical and Polarimetric Radar Platforms," we explored optical sensor data—Landsat Thematic Mapper (TM) images for LULC classification in Altamira by examining the roles of vegetation indices and textural images in improving LULC classification, and by comparing different classification algorithms: MLC, ANN—multilayer perceptron (MLP) trained by back propagation (BP) algorithm, classification tree analysis (CTA), and object-based classification (OBC).[6] We then explored the use of ALOS (Advanced Land Observing Satellite) PALSAR L-band (Phased Array type L-band Synthetic Aperture Radar) and RADARSAT-2 C-band data for LULC classification by examining different textural images which were developed by using the gray-level co-occurrence matrix method based on different polarization options (e.g., HH and HV) and different classification algorithms—MLC, CTA, Fuzzy ARTMAP (a neural-network method), K-nearest neighbor (KNN), OBC, and SVM.[7] Because of different features of Landsat TM and radar data, we explored the integration of Landsat TM and radar images (i.e., ALOS PALSAR L-band and RADARSAT-2 C-band) for LULC classification by comparing different data fusion methods—principal component analysis (PCA), wavelet-merging technique (Wavelet), High Pass Filter resolution-merging (HPF), and normalized multiplication (NMM).[8]

Based on the above research,[6–8] this paper conducted a comprehensive comparison of different classification algorithms and different remote sensing datasets for LULC classification. The new contribution of this paper is to better understand the selection of a classification algorithm suitable for a specific remote sensing data in the moist tropical region of the Brazilian Amazon. Therefore, we selected four typical datasets—Landsat TM multispectral bands, combination of ALOS PALSAR L-band HH and HV images and derived textural images, combination of TM multispectral bands and PALSAR-derived textural images as extra bands, and the multisensor fusion image with wavelet-merging technique, and four typical classification algorithms—MLC, CTA, Fuzzy ARTMAP, and KNN, which include traditional parametric algorithm and nonparametric algorithms for this comparative analysis. The overall goal of this study is to provide some new insights on selection of datasets and associated classification algorithm for LULC classification in the moist tropical region of the Brazilian Amazon.

## 2 Methods

In order to conduct synthetic analysis, it is important to select a study area where different remote sensing and reference datasets are available. Therefore, one of our major study areas—Altamira, which is located along the Transamazon Highway (BR-230) in the northern Brazilian State of Pará, is selected. The study area covers approximately 3110 $km^2$. The dominant native types of vegetation are mature moist forest and liana forest. Deforestation since the early 1970s has led to a complex landscape consisting of different succession stages, pasture, and agricultural lands.[8,9] Different stages of successional forests are distributed along the Transamazon Highway and feeder roads.

The framework of LULC classification for this study is illustrated in Fig. 1. The major contents include (1) collection of sample plots for use as training samples and test samples, respectively; (2) remote sensing data collection and preprocessing; (3) image processing such as development of textural images and data fusion; (4) LULC classification with different algorithms; and (5) evaluation of the classification results.

### 2.1 *Data Collection and Selection of Datasets for LULC Classification*

Different sensor data and field survey data used in this research are summarized in Table 1. The QuickBird image and field survey data were used to develop sample plots. A total of 432 sample

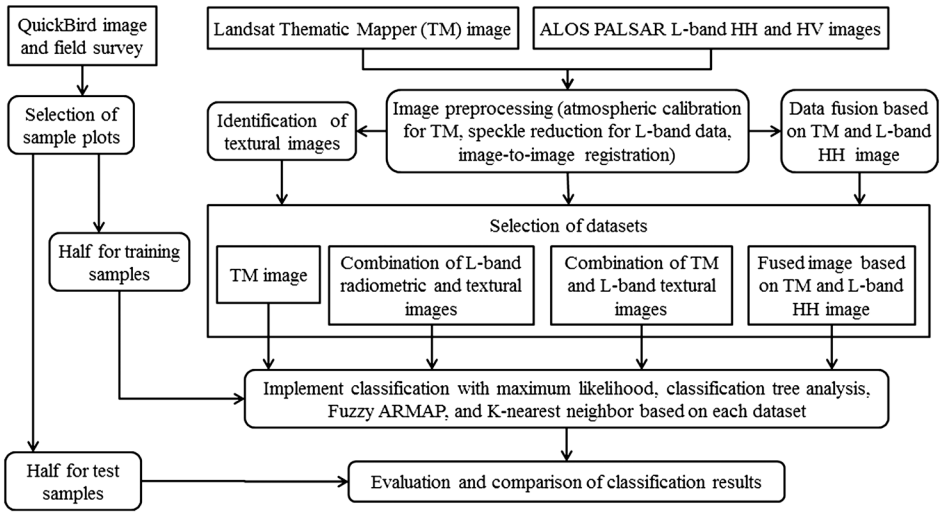


**Fig. 1** Strategy of land use and land cover classification with different algorithms on various datasets.

plots were collected, of which 220 samples were randomly selected (based on the rule of the minimum number of 10 plots for each LULC class) for use as training sample plots in the image classification and the remaining 212 samples for use as test sample plots in accuracy assessment. A LULC classification system consisting of three forest classes (upland, flooding, and liana forests), three succession stages (initial, intermediate, and advanced successional stages), agropasture, and three nonvegetated classes (water, wetland, and urban) were designed. Since agricultural lands and pasture have similar features during dry season, they were grouped into one class called agropasture in this research.

Both Landsat TM and ALOS PALSAR images were registered into Universal Transverse Mercator coordinate system (zone 22, south). An improved image-based dark object subtraction model was used to conduct radiometric and atmospheric correction for Landsat TM image.[10] Based on our previous research,[7] the two best textural images based on the PALSAR L-band HH image were the textures SM25 (second moment with a window size of $25 \times 25$ pixels) and CON31 (contrast with a window size of $31 \times 31$ pixels), and the two best textural images based on the L-band HV image were the textures CON25 (contrast with a window size of $25 \times 25$ pixels) and SM19 (second moment with a window size of $19 \times 19$ pixels). The selected textural images were used in two datasets as extra bands: one was in PALSAR L-band HH and HV images, and another was in TM multispectral image. An alternative to integrate the PALSAR and TM multispectral data is through a fusion technique.[11,12] Our research has indicated that the wavelet-based merging technique can better preserve spectral features in addition to improving spatial resolution.[8] Thus, this technique is used to integrate PALSAR L-band HH band and TM multispectral bands into a new data set with spatial

**Table 1** A summary of datasets used in research.

| Datasets | Brief description |
|---|---|
| Landsat 5 TM image | Multispectral image (six bands covering visible, near-infrared, and shortwave infrared wavelengths) with spatial resolution of 30 m, acquired on July 2, 2008. |
| ALOS PALSAR | FBD (Fine Beam Double Polarization) Level 1.5 products with L-band HH and HV polarization options and 12.5-m pixel spacing, acquired on July 2, 2009. |
| QuickBird imagery | Data fused image consisting of four multispectral bands with spatial resolution of 0.6 m, acquired on June 20, 2008. |
| Field survey data | Fieldwork was conducted in July to August 2009. |

resolution of 10 m in this research. In order to examine the performance of different datasets in LULC classification, four datasets, including (1) Landsat TM multispectral bands; (2) PALSAR L-band data consisting of HH, HV and four textural images; (3) Combination of TM multispectral bands and four PALSAR-derived textural images as extra bands; and (4) Data fusion result based on TM multispectral and PALSAR L-band HH data, were selected.

## 2.2 *Selection of Classification Algorithms and Optimization of Parameters*

In order to identify a suitable classification algorithm for each dataset, one parametric algorithm (i.e., MLC) and three nonparametric algorithms (i.e., CTA, ARTMAP, and KNN) were selected in this research. This is because MLC is the most common parametric classifier and is available in any commercial image processing software, and because CTA, Fuzzy ARTMAP, and KNN may be the most common machine learning algorithms that they have been obtained increasingly attention in the past decade. The major characteristics of these algorithms are summarized in Table 2. Much previous literature has detailed the description of these algorithms.[13–16]

For the nonparametric classification algorithms, one critical step is to identify optimal parameters. In this research, the optimization of relevant parameters used in each nonparametric algorithm was examined separately. In the CTA, different splitting rules—ratio, entropy, and Gini were examined. Another parameter used in this algorithm is to decide whether to use auto-pruning function or not. Use of the auto-pruning function is to eliminate leaves with pixel counts that are less than or equal to a specified proportion within the class. We explored different percentages from 0 to 15% for every 5% interval. For Fuzzy ARTMAP, a small value for choice parameter (default value of 0.01) and relatively high values of learning rate (default value of 1.0) and vigilance parameters (default value of 0.98) in ARTa were recommended. In ARTb, both default learning and vigilance parameters as 1.0 were highly recommended by the Idrisi software. Therefore, the emphasis is on the identification of a suitable choice parameter, learning rate and vigilance parameter in ARTa. For the choice parameter, the values from 0.05 to 0.2 for every interval of 0.05 were tested. For the learning rate, values from 0.5 to 1.0 for every interval of 0.1, and for vigilance parameter, values from 0.94 to 1.0 for every interval of 0.02 were examined. A series of combination of the choice parameter, learning rate and vigilance parameter were tested. For KNN, different $K$ values from 10 to 50 for every 10 interval and different maximum numbers of training samples per class from 50 to 300 for every 50 interval were explored. Table 3 summarized the finally selected parameters for each algorithm.

**Table 2** A summary of major characteristics of the classification algorithms.

| Algorithms | Major characteristics |
|---|---|
| MLC | MLC assumes normal distribution for each feature of interest. It is based on the probability that a pixel belongs to a particular class and takes the variability of classes into account by using the covariance matrix. |
| CTA | CTA is a nonparametric statistical machine learning algorithm, having such advantages as distribution-free and easy interpretation over traditional supervised classifiers. The basic concept of a classification tree is to split a dataset into homogeneous subgroups based on measured attributes. |
| Fuzzy ARTMAP | Fuzzy ARTMAP is a clustering algorithm operating on vectors by a fuzzy set of features, or a pattern of fuzzy membership values between 0 and 1 and consists of four layers of neurons: input, category, mapfield and output. It is controlled by a choice parameter $\alpha$, learning rate parameters $\beta 1$ in ARTa and $\beta 2$ in ARTb, and vigilance parameters $\rho 1$ in ARTa and $\rho 2$ in ARTb. The $\rho 1$ and $\rho 2$ control the operation during learning and operational phases of the network and the mapfield weights and category layer weights are learned adaptively during the process. |
| KNN | KNN is based on the minimum distance from image pixels to the training samples. Euclidean distance is often used to calculate the distance between two pixels. A suitable $k$ value is crucial for a successful classification: a large $k$ value reduces the effect of noise on the classification, but makes boundaries between classes less distinct; a small $k$ value may not result in a good classification accuracy. |

**Table 3** Optimization of parameters used in the nonparametric algorithms for different datasets.

| | | | Selected parameters for each datase | | | |
|---|---|---|---|---|---|---|
| Classifiers | | Parameters | TM | PALSAR | TM_Ltext | Fusion |
| CTA | | Splitting rule | ratio | Gini | ratio | ratio |
| | | Auto-pruning | 0% | 0% | 10% | 5% |
| ARTMAP | ARTa | Choice | 0.01 | 0.01 | 0.01 | 0.01 |
| | | Learning rate | 0.9 | 0.8 | 0.9 | 0.7 |
| | | Vigilance | 0.98 | 0.98 | 0.98 | 0.98 |
| | ARTb | Learning rate (1.0) and vigilance (1.0) recommended by software | | | | |
| KNN | | *K* value | 20 | 30 | 20 | 20 |
| | | Maximum number of training samples/class | 50 | 200 | 250 | 200 |

Note: Four datasets TM, PALSAR, TM_Ltext and Fusion represent (1) Landsat TM multispectral image, (2) ALOS PALSAR L-band HH, HV and selected textural images, (3) combination of Landsat TM multispectral images and PALSAR-derived textural images as extra bands, and (4) fusion results with the wavelet-merging technique based on Landsat TM multispectral bands and PALSAR L-band HH image.

### 2.3 *Evaluation of the Classification Results*

The four classification algorithms were used to classify each dataset into a thematic map consisting of 10 classes using the same training sample plots. In order to identify a best classification algorithm for each dataset, a comparative analysis of the classified images was conducted through the comparison of classification accuracy assessment results. An error matrix approach was used to evaluate the classification results. An error matrix provides detailed assessment of the agreement between the classified result and reference data and provides the information of how misclassification happened.[17] Overall classification accuracy, producer's accuracy, user's accuracy, and kappa coefficient are then calculated from the error matrix.[17] Since both overall classification accuracy and kappa coefficient cannot provide the reliability of each LULC class, producer's accuracy and user's accuracy are often used to provide the complementary analysis of the accuracy assessment. In this study, a total of 212 test sample plots (12 to 33 plots for each LULC class) from the field survey and the 2008 QuickBird image were used for accuracy assessment.

## 3 Results and Discussion

The classification results in Table 4 indicate that no one algorithm is best for each LULC class and no one algorithm is always best for different datasets. Considering overall accuracies and kappa coefficients based on Landsat TM multispectral image, CTA provided the highest accuracy, followed by KNN and MLC, but ARTMAP provided the lowest accuracy. Examining producer's and user's accuracies for individual classes, if the results from MLC were used as basis, the CTA mainly improved classification accuracies of upland forest, initial succession, and agropasture classes; and KNN improved upland forest and initial succession classification accuracies. Although Fuzzy ARTMAP has poorest overall accuracy and reduced the classification accuracies of vegetation succession stages, this algorithm indeed improved nonvegetation land covers. Comparing the results based on Landsat TM multispectral image by using the traditional parametric algorithm—MLC, the nonparametric algorithm—CTA improved overall accuracy by 3.8%.

Comparing with the classification accuracy assessment results from Landsat TM (i.e., overall accuracy values of 79.7% to 84.9%), the PALSAR data have much low overall accuracy values (i.e., overall accuracy of only 47.6% to 59.4%) irrespective of the classification

**Table 4** Comparison of classification results from different classification algorithms for each dataset.

| | MLC | | CTA | | ARTMAP | | KNN | |
|---|---|---|---|---|---|---|---|---|
| | PA | UA | PA | UA | PA | UA | PA | UA |
| | **Landsat TM multispectral data** | | | | | | | |
| Upland forest | 69.7 | 88.5 | 90.9 | 85.7 | 90.9 | 65.2 | 72.7 | 92.3 |
| Flooding forest | 93.3 | 73.7 | 86.7 | 72.2 | 73.3 | 64.7 | 80.0 | 70.6 |
| Liana forest | 83.3 | 71.4 | 75.0 | 81.8 | 58.3 | 100.0 | 83.3 | 58.8 |
| Initial succession | 57.9 | 57.9 | 68.4 | 59.1 | 52.6 | 71.4 | 63.2 | 57.1 |
| Intermediate succession | 87.5 | 75.0 | 75.0 | 78.3 | 79.2 | 70.4 | 83.3 | 83.3 |
| Advanced succession | 85.7 | 85.7 | 81.0 | 94.4 | 33.3 | 63.6 | 95.2 | 74.1 |
| Agropasture | 73.1 | 82.6 | 76.9 | 87.0 | 88.5 | 82.1 | 69.2 | 81.8 |
| Water | 87.5 | 100.0 | 100.0 | 100.0 | 100.0 | 100.0 | 100.0 | 100.0 |
| Wetland | 80.0 | 92.3 | 86.7 | 86.7 | 100.0 | 100.0 | 73.3 | 100.0 |
| Urban | 100.0 | 82.1 | 100.0 | 100.0 | 100.0 | 100.0 | 100.0 | 100.0 |
| Overall accuracy | 81.1 | | 84.9 | | 79.7 | | 82.1 | |
| Kappa coefficient | 0.79 | | 0.83 | | 0.77 | | 0.80 | |
| | **PALSAR L-band HH and HV images and the selected textural images** | | | | | | | |
| Upland forest | 51.5 | 39.5 | 81.8 | 50.0 | 75.8 | 39.7 | 21.2 | 33.3 |
| Flooding forest | 73.3 | 61.1 | 80.0 | 60.0 | 80.0 | 70.6 | 73.3 | 52.4 |
| Liana forest | 25.0 | 15.8 | 16.7 | 25.0 | 16.7 | 100.0 | 25.0 | 14.3 |
| Initial succession | 42.1 | 50.0 | 31.6 | 66.7 | 26.3 | 55.6 | 36.8 | 46.7 |
| Intermediate succession | 66.7 | 64.0 | 58.3 | 77.8 | 45.8 | 64.7 | 54.2 | 32.5 |
| Advanced succession | 23.8 | 38.5 | 14.3 | 25.0 | 23.8 | 38.5 | 19.1 | 26.7 |
| Agropasture | 76.9 | 62.5 | 73.1 | 65.5 | 88.5 | 63.9 | 76.9 | 60.6 |
| Water | 83.3 | 95.2 | 95.8 | 92.0 | 100.0 | 92.3 | 95.8 | 100.0 |
| Wetland | 33.3 | 55.6 | 20.0 | 33.3 | 33.3 | 62.5 | 33.3 | 41.7 |
| Urban | 60.9 | 87.5 | 73.9 | 60.7 | 60.9 | 66.7 | 34.8 | 72.7 |
| Overall accuracy | 56.1 | | 59.4 | | 59.4 | | 47.6 | |
| Kappa coefficient | 0.51 | | 0.54 | | 0.54 | | 0.42 | |
| | **Combination of Landsat TM and PALSAR-derived textural images as extra bands** | | | | | | | |
| Upland forest | 81.8 | 62.8 | 78.8 | 72.2 | 54.6 | 38.3 | 72.7 | 92.3 |
| Flooding forest | 86.7 | 68.4 | 80.0 | 70.6 | 60.0 | 36.0 | 86.7 | 72.2 |
| Liana forest | 66.7 | 88.9 | 83.3 | 83.3 | 0.0 | 0.0 | 83.3 | 71.4 |
| Initial succession | 42.1 | 72.7 | 42.1 | 72.7 | 26.3 | 83.3 | 68.4 | 65.0 |
| Intermediate succession | 87.5 | 80.8 | 70.8 | 81.0 | 41.7 | 52.6 | 79.2 | 86.4 |

**Table 4** (*Continued*).

| | MLC | | CTA | | ARTMAP | | KNN | |
|---|---|---|---|---|---|---|---|---|
| | PA | UA | PA | UA | PA | UA | PA | UA |
| Advanced succession | 38.1 | 80.0 | 61.9 | 68.4 | 19.1 | 33.3 | 100.0 | 75.0 |
| Agropasture | 96.2 | 75.8 | 92.3 | 72.7 | 76.9 | 62.5 | 76.9 | 87.0 |
| Water | 87.5 | 100.0 | 100.0 | 100.0 | 95.8 | 88.5 | 100.0 | 100.0 |
| Wetland | 80.0 | 85.7 | 100.0 | 93.8 | 33.3 | 50.0 | 93.3 | 100.0 |
| Urban | 100.0 | 88.5 | 100.0 | 100.0 | 56.5 | 37.1 | 100.0 | 100.0 |
| Overall accuracy | 78.3 | | 81.1 | | 50.5 | | 85.4 | |
| Kappa coefficient | 0.76 | | 0.79 | | 0.44 | | 0.84 | |
| | **Fusion image from TM and PALSAR L-band HH data** | | | | | | | |
| Upland forest | 75.8 | 89.3 | 78.8 | 86.7 | 90.9 | 88.2 | 78.8 | 92.9 |
| Flooding forest | 93.3 | 70.0 | 93.3 | 63.6 | 93.3 | 73.7 | 86.7 | 72.2 |
| Liana forest | 91.7 | 84.6 | 66.7 | 100.0 | 66.7 | 100.0 | 83.3 | 83.3 |
| Initial succession | 79.0 | 71.4 | 73.7 | 70.0 | 63.2 | 63.2 | 68.4 | 59.1 |
| Intermediate succession | 87.5 | 91.3 | 91.7 | 88.0 | 91.7 | 88.0 | 87.5 | 91.3 |
| Advanced succession | 90.5 | 86.4 | 90.5 | 90.5 | 95.2 | 90.9 | 95.2 | 74.1 |
| Agropasture | 80.8 | 91.3 | 76.9 | 87.0 | 73.1 | 82.6 | 69.2 | 85.7 |
| Water | 87.5 | 100.0 | 91.7 | 100.0 | 100.0 | 96.0 | 95.8 | 100.0 |
| Wetland | 80.0 | 100.0 | 86.7 | 86.7 | 93.3 | 100.0 | 93.3 | 93.3 |
| Urban | 100.0 | 79.3 | 100.0 | 88.5 | 100.0 | 100.0 | 100.0 | 100.0 |
| Overall accuracy | 85.9 | | 85.4 | | 87.7 | | 85.4 | |
| Kappa coefficient | 0.84 | | 0.84 | | 0.86 | | 0.84 | |

Note: (1) PA and UA represent producer's accuracy and user's accuracy. (2) Classification algorithms—MLC, CTA, ARTMAP, and KNN represent maximum likelihood classification, classification tree analysis, Fuzzy ARTMAP, and K-nearest neighbor.

algorithms (see Table 4). For the PALSAR data, CTA and Fuzzy ARTMAP provided relatively better performance, followed by MLC and KNN. The PALSAR data can provide relatively good classification performance for upland forest, flooding forest, agropasture, and water, but very poor performance for liana forest, initial and advanced succession stages, and wetland, implying the potential role of PALSAR data in improving classification performance for certain LULC types if this dataset is properly incorporated into Landsat multispectral image.

For the combination of TM and PALSAR-derived textural images, KNN provided the best performance, followed by CTA, but Fuzzy ARTMAP provided the poorest overall accuracy. Comparing with the accuracy assessment results from both Landsat TM multispectral imagery and the incorporation of TM and PALSAR-derived textural images indicated that KNN improved overall accuracy by 3.3%, which mainly improved flooding forest, liana forest, initial succession, advanced succession and agropasture classes. In contrast, the rest classification algorithms reduced overall classification accuracies. Because PALSAR data have poor classification performance for upland forest, liana forest, initial and advanced succession and wetland, direct combination of PALSAR data as extra bands into Landsat multispectral bands

cannot increase much complementary information in helping improve the separability of vegetation types. As image dimension increased, Fuzzy ARTMAP became especially difficult in optimizing the parameters as the training process became prohibitively long. Because the assumption of normal distribution is not satisfied in the combination of TM multispectral and PALSAR-derived textural images, the MLC has reduced its overall performance by 2.8%, as shown in Table 4.

Comparing with the Landsat TM image classification results, the wavelet-based fusion imagery improved overall classification performance irrespective of the classification algorithms, that is, the selected algorithms based on data fusion images provided overall accuracies of 85.4% to 87.7% comparing with 79.7% to 84.9% based on TM imagery. This situation implies the importance of improved spatial resolution and the integration of different data features in the fusion image for LULC classification. Because PALSAR data have different features in reflecting land surfaces, especially in vegetation structure and moist contents, integration of PALSAR data with Landsat multispectral image with the wavelet-merging technique proved valuable in improving classification performance of vegetation types.

A comparison of kappa coefficients from different classification algorithms and from different datasets (Fig. 2) indicates that the TM multispectral image and the multisensor fusion image provided reliable and stable classification results irrespective of classification algorithms. Overall, the multisensor fusion image had better classification performance than the TM multispectral image. The combination of TM and PALSAR-derived textural images as extra bands provided better classification performance than the TM multispectral image only when KNN was used. In contrast, the Fuzzy ARTMAP provided poorest classification results for this dataset. The major reason is that the addition of PALSAR-based textural images did not improve separability of

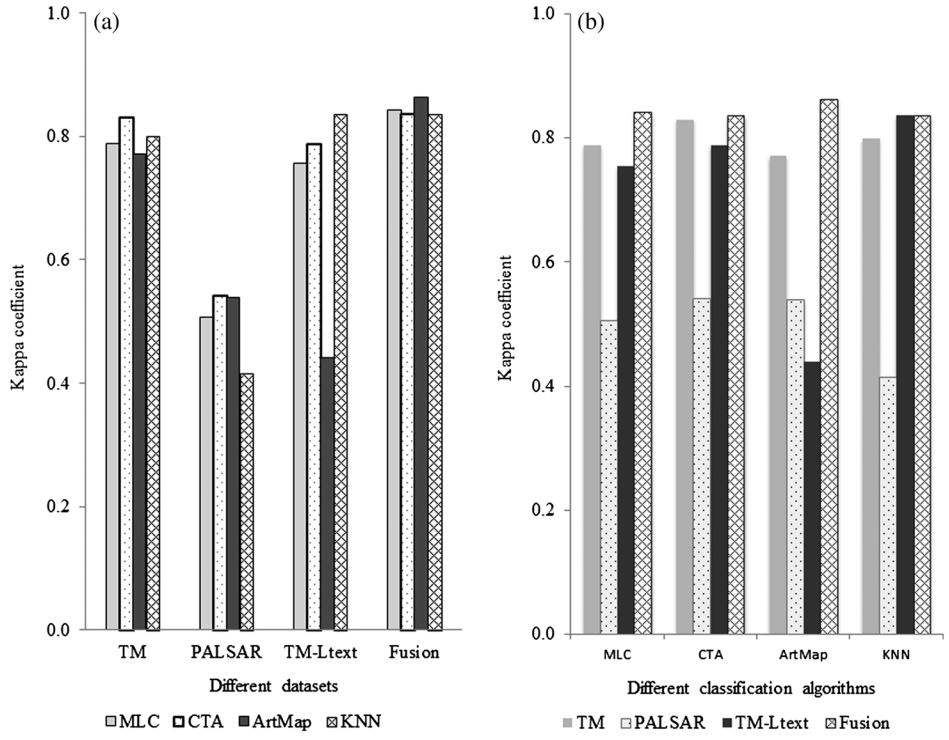


**Fig. 2** A comparison of kappa coefficients among different classification methods and among different datasets in the Brazilian Amazon. Note: Four datasets TM, PALSAR, TM_Ltext and Fusion represent (1) Landsat TM multispectral image, (2) ALOS PALSAR L-band HH, HV and selected textural images, (3) combination of Landsat TM multispectral images and PALSAR-derived textural images as extra bands, and (4) fusion results with the wavelet-merging technique based on Landsat TM multispectral bands and PALSAR L-band HH image. Classification algorithms—MLC, CTA, ARTMAP, and KNN represent maximum likelihood classification, classification tree analysis, Fuzzy ARTMAP, and K-nearest neighbor.

different vegetation types and more image bands make much more difficult in determining optimal parameters due to the prohibitive time required during the training process. Overall, ALOS PALSAR data had much poorer classification results than TM multispectral image, implying its incapability in classifying the detailed LULC classification system. This research indicates that TM spectral feature is still the most important data source for LULC classification, but properly integrating PALSAR data into TM multispectral image is valuable for improving vegetation classification performance. In addition to the selection of datasets, selection of a suitable classification algorithm corresponding to the specific dataset is also valuable. When the remote sensing data meet the normal distribution requirement, MLC can provide reliable classification results, although some nonparametric algorithms such as CTA for Landsat TM and Fuzzy ARTMAP for the fusion image can improve classification performance. For the remote sensing datasets such as PALSAR data and the combination of TM multispectral and PALSAR-derived textural images, the assumption of normal distribution is often violated, thus nonparametric algorithms such as CTA for PALSAR data and KNN for the combination of TM and PALSAR data provide better performance than MLC.

The nonparametric algorithms often require much longer time during the classification procedure than MLC because of the requirement in optimizing parameters used in nonparametric algorithms. For example, ARTMAP requires lengthy trials for identifying optimized parameters as learning rate and vigilance parameter, and this is especially true when many bands are used for detailed LULC classification. CTA and KNN require much less time for image classification compared with ARTMAP because of less number of parameters used in these algorithms. On the other hand, lack of clear and standardized guidelines for the determination of the parameters requires much experimentation by the analyst. This research also indicates that no single classification algorithm is perfect for each LULC type, but that each has its own merits. Therefore, it is important to develop new methods to combine the merits of different algorithms to produce a new classification result with high classification accuracy for each LULC type.[18,19]

## 4 Conclusions

This study showed that LULC classification accuracies varied considerably depending on the dataset used in the classification procedure and the selected classification algorithm. Overall, MLC provided reasonably good classification accuracy for the TM multispectral image and multisensor fusion image and required much less time during the classification procedure than the nonparametric classification algorithms. Some nonparametric classification algorithms can provide better classification than MLC, but required much longer times for the classification procedure. In particular, Fuzzy ARTMAP required the longest time periods during the training process and for optimization of parameters. When the number of LULC classes and the number of image bands are large, the Fuzzy ARTMAP takes a prohibitive time period during training process. Both CTA and KNN require much less time for the optimization of parameters than Fuzzy ARTMAP. Considering the selection of datasets, integration of Landsat multispectral and ALOS PALSAR data with the wavelet-merging technique is valuable in improving vegetation classification in the moist tropical region. This research provides valuable information for guiding the selection of remote sensing dataset and classification algorithms for LULC classification, especially in moist tropical regions.

## Acknowledgments

The authors thank National Science Foundation (Grant #BCS 0850615) for funding this research. Sidnei J.S. Sant'Anna thanks JAXA (AO 108) Science Program for providing the ALOS PALSAR data used in this research. We also thank Anthony Cak for his assistance in the fieldwork and Scott Hetrick for his assistance in organizing the field data. Any opinions, findings, and conclusions or recommendations expressed in this material are those of the authors and do not necessarily reflect the views of the National Science Foundation.

## References


1. D. Lu and Q. Weng, "A survey of image classification methods and techniques for improving classification performance," *Int. J. Remte Sens.* **28**(5), 823–870 (2007), http://dx.doi.org/10.1080/01431160600746456.
2. J. Rogan et al., "Mapping land-cover modifications over large areas: a comparison of machine learning algorithms," *Remote Sens. Environ.* **112**(5), 2272–2283 (2008), http://dx.doi.org/10.1016/j.rse.2007.10.004.
3. Y. Shao and R. S. Lunetta, "Comparison of support vector machine, neural network, and CART algorithms for the land-cover classification using limited training data points," *ISPRS J. Photogram. Remte Sens.* **70**, 78–87 (2012), http://dx.doi.org/10.1016/j.isprsjprs.2012.04.001.
4. P. K. Srivastava et al., "Selection of classification techniques for land use/land cover change investigation," *Adv. Space Res.* **50**(9), 1250–1265 (2012), http://dx.doi.org/10.1016/j.asr.2012.06.032.
5. B. Tso and P. M. Mather, *Classification Methods for Remotely Sensed Data*, p. 356, Taylor & Francis, London (2009).
6. G. Li et al., "Land-cover classification in a moist tropical region of Brazil with Landsat TM imagery," *Int. J. Remote Sens.* **32**(23), 8207–8230 (2011), http://dx.doi.org/10.1080/01431161.2010.532831.
7. G. Li et al., "A comparative analysis of ALOS PALSAR L-band and RADARSAT-2 C-band data for land-cover classification in a tropical moist region," *ISPRS J. Photogramm. Remote Sens.* **70**, 26–38 (2012), http://dx.doi.org/10.1016/j.isprsjprs.2012.03.010.
8. D. Lu et al., "A comparison of multisensor integration methods for land-cover classification in the Brazilian Amazon," *GISci. Remote Sens.* **48**(3), 345–370 (2011), http://dx.doi.org/10.2747/1548-1603.48.3.345.
9. E. F. Moran and E. S. Brondízio, "Land-use change after deforestation in Amazônia," in *People and Pixels: Linking Remote Sensing and Social Science*, D. Liverman, E. F. Moran, R. R. Rindfuss, and P. C. Stern, Eds., pp. 94–120, National Academy Press, Washington, D.C. (1998).
10. G. Chander, B. L. Markham, and D. L. Helder, "Summary of current radiometric calibration coefficients for Landsat MSS, TM, ETM+, and EO-1 ALI sensors," *Remote Sens. Environ.* **113**(5), 893–903 (2009), http://dx.doi.org/10.1016/j.rse.2009.01.007.
11. M. Ehlers et al., "Multisensor image fusion for pansharpening in remote sensing," *Int. J. Image Data Fusion* **1**(1), 25–45 (2010), http://dx.doi.org/10.1080/19479830903561985.
12. J. Zhang, "Multisource remote sensing data fusion: status and trends," *Int. J. Image Data Fusion* **1**, 5–24 (2010), http://dx.doi.org/10.1080/19479830903561035.
13. M. Zambon et al., "Effect of alternative splitting rules on image processing using classification tree analysis," *Photogram. Eng. Remote Sens.* **72**(1), 25–30 (2006).
14. R. R. McRoberts and E. O. Tomppo, "Remote sensing support for national forest inventories." *Remote Sens. Environ.* **110**(4), 412–419 (2007), http://dx.doi.org/10.1016/j.rse.2006.09.034.
15. T. Islam et al., "Artificial intelligence techniques for clutter identification with polarimetric radar signatures," *Atmos. Res.* **109–110**, 95–113 (2012), http://dx.doi.org/10.1016/j.atmosres.2012.02.007.
16. Y. Zhong and L. Zhang, "An adaptive artificial immune network for supervised classification of multi-/hyperspectral remote sensing imagery," *IEEE Trans. Geosci. Remote Sens.* **50**(3), 894–909 (2012), http://dx.doi.org/10.1109/TGRS.2011.2162589.
17. R. G. Congalton and K. Green, *Assessing the Accuracy of Remotely Sensed Data: Principles and Practices*, 2nd ed., p. 183, CRC Press, Taylor & Francis Group, Boca Raton, Florida (2008).
18. S. Chitroub, "Classifier combination and score level fusion: concepts and practical aspects," *Int. J. Image Data Fusion* **1**(2), 113–135 (2010), http://dx.doi.org/10.1080/19479830903561944.
19. D. Zhu, "A hybrid approach for efficient ensembles," *Decis. Support Syst.* **48**(3), 480–487 (2010), http://dx.doi.org/10.1016/j.dss.2009.06.007.

**Guiying Li** is currently a postdoctoral fellow at Indiana University. She received her PhD in physical geography from Indiana State University in 2008. Her research interests include remote sensing, LULC change, urban environment, and forestry.

**Dengsheng Lu** is currently a professor at the Center for Global Change and Earth Observations, Michigan State University. He received his PhD in physical geography from Indiana State University in 2001. He worked at Indiana University as a postdoctoral fellow and assistant research scientist in 2001 to 2006 and as associate scientist and then senior scientist in 2008 to 2012, and worked at Auburn University as research fellow in 2007 to 2008. He is the author of over 60 peer-reviewed journal articles and book chapters. His research interests include LULC change, biomass/carbon estimation, and urban-environmental interactions.

**Emilio Moran** is a distinguished professor at Indiana University, and has been a leader for nearly two decades in the integration of remote sensing with social science questions, in developing approaches to classifying secondary succession in the Amazon, and in LUCC (land use and land cover change). He was cochair of the Global Land Project Transition Team that prepared the Science Plan, and was leader of Focus 1 of LUCC before that for over five years. He was PI on a Center-level grant from NSF from 1996 to 2006 from SBE in support of CIPEC, a center of excellence on the human dimensions of global environmental change. He has also been PI on NASA, NIH and NOAA grants. He is the author of nine books, 14 edited volumes and over 140 journal articles and book chapters. He was elected to the National Academy of Sciences in 2010.

**Sidnei João Siqueira Sant'Anna** received a BS degree in electrical and electronic engineering from the Universidade Federal do Rio de Janeiro in 1993, the MSc degree in remote sensing from the Instituto Nacional de Pesquisas Espaciais (INPE), São José dos Campos, Brazil in 1995 and a PhD degree in electronic engineering and computing from the Instituto Tecnológico de Aeronáutica (ITA), São José dos Campos, Brazil, in 2009. He is currently a technologist at INPE, and his interests are image analysis and processing techniques for remote sensing (SAR image filtering, statistical methods, robustness, etc.).